Current Applied Physics 10 (2010) 526–530

Contents lists available at ScienceDirect

Current Applied Physics

journal homepage: www.elsevier.com/locate/cap

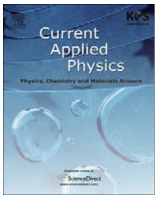

Double hysteresis loops induced by Mn doping in $Pb_{0.99}Nb_{0.02}(Zr_{0.95}Ti_{0.05})_{0.98}O_3$ ferroelectric ceramics

Meng Jiang [a], Xuhai Li [a], Jiliang Zhu [a,*], Xiaohong Zhu [b], Wei Shi [a], Lihua Li [a], Dingquan Xiao [a], Jianguo Zhu [a]

[a] *Department of Materials Science, Sichuan University, Chengdu 610064, China*
[b] *CEA-LETI MINATEC, 17 Rue des Martyrs, 38054 Grenoble Cedex 9, France*

ARTICLE INFO

Article history:
Received 3 May 2009
Received in revised form 8 July 2009
Accepted 13 July 2009
Available online 16 July 2009

PACS:
77.80.−e
77.84.Dy
77.90.+k

Keywords:
PNZT95/5
Antiferroelectric
Double hysteresis loops
Defect dipoles

ABSTRACT

$Pb_{0.99}Nb_{0.02}(Zr_{0.95}Ti_{0.05})_{0.98}O_3$ (PNZT95/5) ceramics with 1 mol% and without Mn doping were prepared via conventional solid state reaction process. X-ray diffraction patterns show that the PNZT95/5 and Mn-doped PNZT95/5 (PNZTM95/5) ceramics, with composition near the boundary of the ferroelectric phase (FE)/antiferroelectric phase (AFE), have a rhombohedral perovskite structure. The ferroelectric behavior of PNZT95/5 ceramics is strongly affected by Mn doping. Without any aging process the PNZTM95/5 ceramics possess double hysteresis loops (*P*–*E* loops), whereas the PNZT95/5 ceramics possess normal single hysteresis loops. Due to the defect dipoles formed by effectively negatively charged Mn^{3+} dopants and positively charged O^{2-} vacancies, the PNZTM95/5 ceramics exhibit the double *P*–*E* loops. The defect dipole effect has been proved by investigating the *P*–*E* loops under different external fields. As a result, the PNZTM95/5 ceramics become "hardened", exhibiting a high mechanical quality factor (1300).

1. Introduction

Double hysteresis loops (*P*–*E* loops) are an exceptional phenomenon in ferroelectrics (FE), which are often observed in antiferroelectric (AFE) materials such as the Zr-rich $Pb(Zr_{1-x}Ti_x)O_3$ (PZT) ceramics because of the neighboring lines polarized in antiparallel directions [1–5]. In the Zr-rich family, $Pb(Zr_{0.95}Ti_{0.05})O_3$ (PZT95/5) near the boundary of FE/AFE is of technological importance due to its wide applications in micro-electromechanical systems and energy storage devices [1–4]. Then, a particularly interesting member in the PZT95/5 family is the $Pb_{0.99}Nb_{0.02}(Zr_{0.95}Ti_{0.05})_{0.98}O_3$ (PNZT95/5). A small amount of Nb substitution can stabilize the FE phase and reduce the dielectric losses [2]. And it is also a mature material for studying the FE/AFE phase transition. As a matter of fact, in the acceptor doped ferroelectric materials (mainly in $BaTiO_3$) double hysteresis loops can also be observed [6–11]. Based on the symmetry-conforming principle of point defects, the domain stabilization is a volume effect in the ferroelectrics [12]. This theory could well explain the differences of the *P*–*E* loops between the acceptor doped ferroelectric and the normal ferroelectric [5,12,13]. Ren et al. has suggested that in the acceptor element Mn doped $BaTiO_3$, the defect ions Mn^{3+} and the O^{2-} vacancies form defect dipoles to pin the migration of ferroelectric dipoles and induce double hysteresis loops [6,12]. Although the defect dipoles induced double loops are often observed in the conventional ferroelectrics like $BaTiO_3$, there is little work about similar characteristics in the PZT family, especially near the FE/AFE boundary. In this work, we report the observation of double loop phenomenon in 1 mol% Mn-doped PNZT95/5 (denoted as PNZTM95/5) ceramics and the resulting effects on the electromechanical and dielectric properties of the ceramics.

2. Experimental procedure

The PNZT95/5 and PNZTM95/5 ceramics, respectively, were synthesized by a solid-state reaction process using metal oxides or carbonate powders: PbO (99%), ZrO_2 (99%), Nb_2O_5 (99.5%), TiO_2 (99%), and $MnCO_3$ (98%). Raw materials with the proper ratio were mixed by ball milling in ethanol with zirconium media for 24 h, and then calcined at 850 °C in air for 3 h to synthesize the powders. With a little organic binder polyvinyl alcohol (PVA), the powder was pressed into pellets with 1 mm in thickness and 10 mm in diameter under 20 MPa. The compacts were sintered at 1250–1300 °C for 2 h in the PbO atmosphere. Silver paste was sintered on both sides of the samples at 700 °C for 10 min to form the electrodes for electrical measurements.

---

[*] Corresponding author. Tel./fax: +86 28 85432078.
E-mail addresses: jlzhu167@yahoo.com.cn (J. Zhu), xhzhu2006@gmail.com (X. Zhu).

1567-1739/$ - see front matter © 2009 Elsevier B.V. All rights reserved.
doi:10.1016/j.cap.2009.07.012

X-ray diffraction (XRD) analysis was examined using Philips X' Pert Pro X-ray diffractometer with Cu K_α radiation. The polarization versus electric field (P–E) hysteresis loops of the ceramics were measured using a Radiant Precision Workstation (USA). The ceramic samples were poled in a 120 °C silicon oil bath by applying the direct current (dc) electric field of 60 kV/cm for 1 h. The piezoelectric properties, such as electromechanical coupling factor (k_p) and mechanical quality factor (Q_m), and dielectric properties, such as dielectric permittivity (ε_r), of the ceramics were measured with an Agilent 4294A Precision Impedance Analyzer.

3. Results and discussion

Fig. 1 shows the XRD patterns of the PNZT95/5 and PNZTM95/5 ceramics, respectively. Both ceramics exhibit rhombohedral perovskite structure, and the lattice parameters are shown in Table 1. A small change in their lattice parameters is found; the lattice volume of PNZTM95/5 is smaller than that of PNZT95/5. It suggests that Mn has diffused into the PNZT95/5 lattice. From the enlarged XRD patterns of the ceramics in the 2θ range of 37.5–38.5°, 53.5–55.5°, and 62.5–64.5°, there are two splitting peaks in the PNZT95/5 ceramics. However, the two splitting peaks are incorporated in the PNZTM95/5 ceramics. Being very near to the FE/AFE phase boundary, PNZT95/5 has been known to be in the ferroelectric phase at room temperature [5]. It is reasonable to speculate that the PNZT95/5 and PNZTM95/5 ceramics belong to the ferroelectric phase at room temperature.

Fig. 2 shows the P–E loops of the PNZT95/5 and PNZTM95/5 ceramics, measured at 10 Hz and room temperature. The two P–E loops are obviously different, as shown in the figure. The PNZT95/5 ceramics possess a relatively large P_r (31 μC/cm^2) and low coercive field E_c (10.4 kV/cm), and show a normal single loop. Coherent with the XRD patterns, the single loop of PNZT95/5 provides an additional evidence for the conclusion that PNZT95/5 belongs to ferroelectric phase. However, the P–E loop of PNZTM95/5 shows a double loop character. The P_r (2.48 μC/cm^2) of the PNZTM95/5 is relatively lower. As mentioned above, the double hysteresis loop of PNZTM95/5 can not be interpreted by the antiferroelectric mechanism; the second possible reason is the acceptor doping induced defect dipoles in ferroelectrics [8]. In fact, recent electron paramagnetic resonance measurements revealed that even with Nb doping, Mn^{2+} and Mn^{4+} exist at very low concentration, thus Mn^{3+} predominates [14]. Similar to the Mn-doped $BaTiO_3$ ceramics, it is obvious that the electrovalence of the Mn^{3+} dopant ions is lower than that of the B-site ions Zr/Ti^{4+}. The non-centric distribution of dopant ions form defect dipoles (effectively positively charged O^{2-} vacancies and negatively charged dopant ions, Mn^{3+} substituted for Zr/Ti^{4+}), and based on the symmetry-conforming principle of point defects, defect dipoles tend to align along the spontaneous polarization direction [6]. Because of the low migration rate of defects, the defect dipoles remain in the original orientation during the P–E loop measurement, which provides a restoring force to reverse the switched polarization and, thus, induces the constricted loops [6,7,11,12].

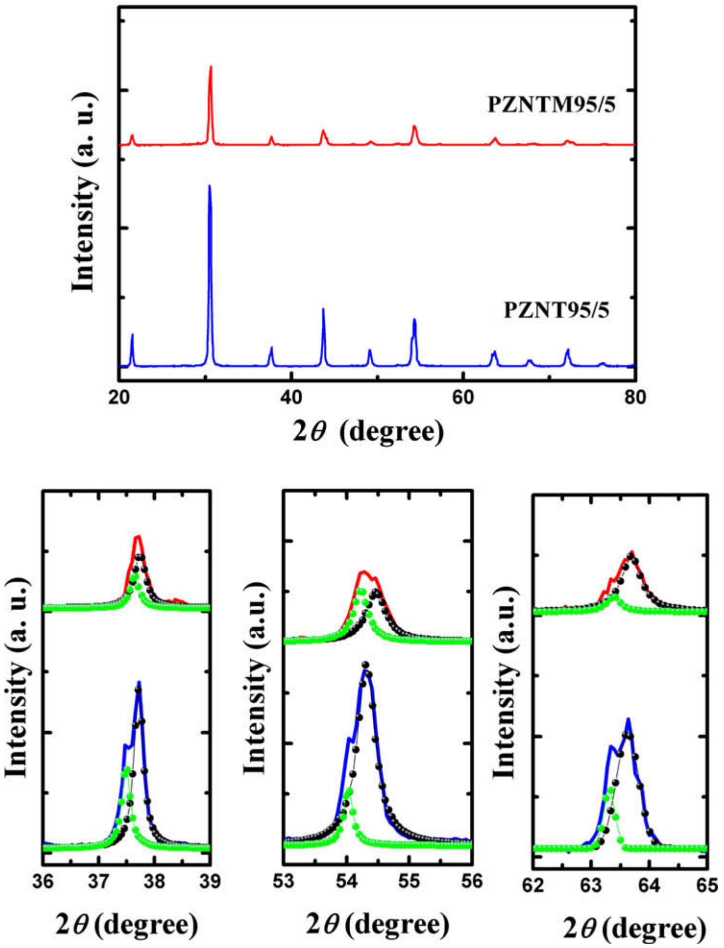

Fig. 1. RD patterns of PNZT95/5 and PNZTM95/5 ceramics, and the corresponding expanded XRD patterns in the 2θ range of 36–39°, 53–56°, and 62–65°.